SUPPLEMENTAL INFORMATION

PRC1 preserves epidermal tissue integrity independently of PRC2

Idan Cohen, Dejian Zhao, Gopinathan Menon, Manabu Nakayama, Haruhiko Koseki,

Deyou Zheng, and Elena Ezhkova

List:

Supplemental Materials and Methods

Transmission electron microscopy

Transmission electron microscopy (TEM) was performed in the Core Pathology Electron Microscopy Facility, Icahn School of Medicine at Mount Sinai. Back skin tissues from E18.5 *Ring1a/b* 2KO, *Eed* cKO and matching controls were fixed in 0.1M sodium cacodylate buffer containing 1% PFA and 3% glutaraldehyde. Samples were post-fixed with 1% osmium tetroxide, dehydrated through a graded series of ethanol, and embedded in Epon (Electron Microscopy Sciences). Ultrathin sections were cut on a Leica Ultracut UCT ultramicrotome, stained with uranyl acetate and lead citrate, and imaged using the Hitachi H7650 microscope.

Epidermal barrier assay

Whole-mount dye-exclusion epidermal permeability barrier assay was performed on P0 pups. Newborn pups were immersed in X-gal solution ((1mg/ml Xgal in 1x phosphate buffered saline (PBS), containing 100 mM $NaPO_4$, 1.3 mM $MgCl_2$, 3mM $K_3Fe(CN)_6$ and 3mM $K_4Fe(CN)_6$; pH=4.5)) overnight at 37 ºC, rotating. Pups were then washed twice with 1x PBS.

Fluorescence-activated cell sorting

P0 back skins from *Eed* cKO, *Ring1a/b* 2KO and control mice were collected and subjected to 0.25% collagenase digestion for 60 minutes at 37ºC with 80 rpm shaking, or incubated in 1.26U/ml dispase (Invitrogen) for 4-6 hours at 4ºC to separate the epidermis from the underlying dermis. Samples were then dissociated by 0.25% Trypsin with 2.21mM EDTA (Corning Cellgro; Manassas, VA, USA) and the cell suspension was washed twice with 1x PBS. Cells were stained with SCA1-PE (1:200; Biolegend), α6-integrin-FITC (1:00; eBiosciences), and EPCAM-APC (1:200; Biolegend) for 30 minutes on ice, and washed twice with 1x HBSS prior to cell sorting. Interfollicular epidermis, enriched for epidermal progenitors, was sorted as EPCAM(+), SCA1(+), and α6-integrin(high). To

validate the enrichment for epidermal progenitors, “whole epidermis” samples were used as controls for comparison. P0 back skins from control mice were incubated in 1.26U/ml dispase (Invitrogen) for 4-6 hours at 4ºC. The epidermis was gently peeled from the underlying dermis, dissociated by 0.25% Trypsin with 2.21mM EDTA and the cell suspension was washed twice with 1x PBS. Pre-sorted epidermal cells were considered as “whole epidermis” samples. All cell isolations were performed on a FACS Influx instrument (BD, Franklin Lakes, NJ, USA) in the Flow Cytometry Core Facility at Icahn School of Medicine at Mount Sinai.

Immunofluorescence staining, microscopy, and staining quantifications

Back skin tissues were collected from mice, embedded in OCT compound (Tissue-Tek, Torrance, CA, USA), and subsequently cut into 7µm sections using a Leica Cryostat. Slides were then pre-fixed in 4% PFA for 10 minutes at room temperature and blocked overnight at 4ºC in blocking solution (1x PBS supplemented with 0.1% Triton X-100, 1% BSA, 0.25% normal donkey serum, 0.01% gelatin). Primary antibodies were diluted in blocking solution and incubated with slides for 1 hour at room temperature, followed by 1-hour incubation with secondary antibodies at room temperature. All antibodies and dilutions are available in Supplemental Table S4. Slides were counterstained with DAPI to visualize nuclei. For detection of apoptosis, TUNEL apoptosis detection assay was performed using the In Situ Cell Death Detection Kit, Fluorescein (Roche). Slides were imaged using a Leica DM5500 slide microscope using 10x, or 20x objectives.

To quantify the relative intensity of the staining, the signals for immunofluorescence were obtained from single color greyscale images and analyzed using the Leica LAS AF software (Leica Microsystems). Background levels of fluorescence were measured in non-epithelial regions of the dermis in the same image.

RNA purification, cDNA preparation and RT-qPCR

FACS-purified epidermal cells were collected directly into RLT Plus buffer and total RNA was isolated using RNeasy Plus Micro Kit (QIAGEN). Total RNA was reverse-transcribed using qScript cDNA SuperMix (Quanta Biosciences, Gaithersburg, MD, USA) according to the manufacturer's instructions. Complimentary DNA (cDNA) samples were analyzed by RT-qPCR using LightCycler® 480 SYBR Green I Master Mix (Roche Diagnostics) on a Lightcycler 480 instrument (Roche). Results were normalized to Ppib mRNA levels. Primer sequences are available in Supplemental Table S4.

Chromatin immunoprecipitation and ChIP-qPCR

Chromatin immunoprecipitation (ChIP) was performed on FACS-sorted populations as previously described (Cohen et al. 2018). Briefly, prior to cell sorting, cells were stained for viability using Zombie violet (Biolegend; San Diego, CA), then cross-linked with 1% formaldehyde (Thermo Fisher Scientific; Rockford, IL) in 1X PBS for 10 minutes at room temperature. Crosslinking was stopped by the addition of 125mM Glycine for 5 minutes at room temperature, and cells were then washed twice with 1x PBS. Cells were incubated in lysis buffer 1 (50mM HEPES pH=7.5, 140mM Nacl, 1mM EDTA, 10% glycerol, 0.5% NP-40, 0.25% Triton X-100, protease inhibitor cocktail (Roche)) for 10 minutes on ice, followed by 10 minutes incubation with lysis buffer 2 (10mM Tris-HCl pH=7.5, 200mM NaCl, 1mM EDTA, 0.5mM EGTA). Cells were then resuspended in lysis buffer 3 (10mM Tris-HCl pH=8.0, 200mM NaCl, 1mM EDTA, 0.5mM EGTA, 0.1% Na-deoxycholate, 0.5% N-laurylsarcosine, 1% Triton X-100) and sonicated using a Branson sonifier at 25% power output for 15 cycles of 30 seconds sonication followed by 90 seconds of rest in ice bath. Chromatin from approximately 0.5 x 10^6 cells was used for H3K27me3, H2AK119ub and H3K27ac ChIP, and chromatin from 6 x 10^6 cells was used for RING1B, and RYBP ChIP. Chromatin was incubated overnight at 4ºC with antibodies as indicated in Supplemental Table S4. Dynal protein G magnetic beads (Invitrogen) were added the next day and incubated for 6 hours. The beads were sequentially washed with low salt, high salt, LiCl, and Tris-EDTA buffers for 10 minutes each at 4ºC. Bound chromatin was eluted and crosslinking was reversed

by overnight incubation at 65ºC, followed by RNase A (Sigma-Aldrich) and proteinase K (Roche Diagnostics) treatments. Samples were purified using the ChIP DNA Clean and Concentrator kit (Zymo Research; Irvine, CA), and were analyzed by qPCR using LightCycler® 480 SYBR Green I Master Mix (Roche Diagnostics) on a Lightcycler 480 instrument (Roche). Primer sequences for ChIP-qPCR are available in Supplemental Table S4.

ChIP-seq data analysis

ChIP-seq data for RING1B, RYBP, BMI1, H3K27me3, H2AK119ub and H3K27ac, in epidermal progenitors were described previously (Cohen et al. 2018) and obtained from the Gene Expression Omnibus (GEO) database (GSE112403, GSE112450). Data analysis was performed as previously described (Cohen et al. 2018). Briefly, the ChIP-seq reads were trimmed by 3 bases at the 5' end using Trim Galore (v0.4.1; http://www.bioinformatics.babraham.ac.uk/projects/trim_galore/), and aligned to the reference genome (mm10) using either bowtie v1.1.1 (Langmead et al. 2009), or bowtie2 v2.2.3 (Langmead and Salzberg 2012). Uniquely aligned reads were kept for downstream analysis, with duplicate reads removed by the Samtools software v0.1.19 (Li et al. 2009), and ChIP-seq kit specific artifacts removed by SMART cleaner (https://github.com/dzhaobio/SMARTcleaner). Peaks for RING1B and H3K27me3 were called as previously described (Goldberg et al. 2010). Peaks called from the two biological replicates were merged to generate a union list of peaks. To visualize ChIP-seq signal, we used the Integrative Genomics Viewer (IGV; (Robinson et al. 2011)) and TDF files from the igvtools v2.3.57 (Thorvaldsdottir et al. 2013).

RNA-seq data analysis

RNA-seq data of P0 *Eed* cKO, *Ring1a/b* 2KO, and control samples enriched for epidermal progenitors was obtained from our previous publication (Cohen et al. 2018), and the GEO database (GSE112382, GSE112402), and data analysis was done as previously described (Cohen et al. 2018).

Briefly, the RNA-seq reads were aligned using Tophat v2.0.13 (Trapnell et al. 2009) to the mouse reference genome (mm10), with gene models of Refgene were downloaded from the UCSC genome browser. FPKM (Fragments Per Kilobase of transcript per Million mapped reads) values were generated using cufflinks v2.2.1 (Trapnell et al. 2010). Genes with low or no expression (mean FPKM values < 1 in both groups under comparison) were excluded from our differential gene expression analysis, and read counts from the HTSeq v0.6.1 (Anders et al. 2015) were used for differential analysis with the DESeq2 v1.6.3 (Love et al. 2014). Genes with absolute fold change >1.8 and false discovery rate (FDR) < 0.05 were considered as significantly differentially expressed.

Gene Ontology enrichment analysis

Identification of significantly over-represented functional categories was done using the DAVID (Huang da et al. 2009). Genes significantly upregulated in *Eed* cKO vs. control epidermis were annotated and selected GO terms are shown in Figure 3A and Supplemental Table S2. Genes significantly upregulated in *Ring1a/b* 2KO vs. control epidermis were annotated and selected GO terms are shown in Figure 3B and Supplemental Table S2. Genes significantly downregulated in *Ring1a/b* 2KO vs. control epidermis were annotated and selected GO terms are shown in Figure 3E and Supplemental Table S2. Selected GO terms were considered significant with $p<0.05$.

STRING protein-protein interaction analysis

Protein-protein interaction connectivity network for genes related to cell adhesion and cytoskeleton organization that were significantly downregulated in *Ring1a/b* 2KO vs. control epidermis was generated using the Search Tool for the Retrieval of Interacting Genes ((STRING V10.5; https://string-db.org/ (Szklarczyk et al. 2015)). Confidence interaction score threshold was set at 0.7 (high confidence), using k-means clustering method with 5 clusters.

Statistics

To determine the statistical significance between two groups, two-sided t test or Mann-Whitney tests were performed. Box-and-whisker boxplots in Figure S5B are minimum-to-maximum: midline, median; box limits, 25th percentile (lower quartile) and 75th percentile (upper quartile); upper whisker, 75th-100th percentile; lower whisker, 0-25th percentile. For boxplots in Figure S5C: midline, median; box limits, 25th percentile (lower quartile) and 75th percentile (upper quartile); upper whisker, 75th-95th percentile; lower whisker, 5th-25th percentile. Scatter plots in Figures S3F and S3H present all data as individual dots, with error bars indicating mean ±SD. Unless indicated otherwise in the figure legends, all data in bar graphs are presented as mean ±SEM. The number of biological replicates used for comparison is indicated for each figure in figure legends. For each comparison, at least 3 animals for each group from two independent litters were used. Significance levels were defined as *p<0.05; **p<0.01; ***p<0.001; NS, not significant. For statistical analyses GraphPad Prism 5 was used.

`

Supplemental References

Anders S, Pyl PT, Huber W. 2015. HTSeq--a Python framework to work with high-throughput sequencing data. *Bioinformatics* **31**: 166-169.

Cohen I, Zhao D, Bar C, Valdes VJ, Dauber-Decker KL, Nguyen MB, Nakayama M, Rendl M, Bickmore WA, Koseki H et al. 2018. PRC1 Fine-tunes Gene Repression and Activation to Safeguard Skin Development and Stem Cell Specification. *Cell Stem Cell* **22**: 726-739 e727.

Goldberg AD, Banaszynski LA, Noh K-M, Lewis PW, Elsaesser SJ, Stadler S, Dewell S, Law M, Guo X, Li X et al. 2010. Distinct Factors Control Histone Variant H3.3 Localization at Specific Genomic Regions. *Cell* **140**: 678-691.

Huang da W, Sherman BT, Lempicki RA. 2009. Systematic and integrative analysis of large gene lists using DAVID bioinformatics resources. *Nat Protoc* **4**: 44-57.

Langmead B, Salzberg SL. 2012. Fast gapped-read alignment with Bowtie 2. *Nat Methods* **9**: 357-359.

Langmead B, Trapnell C, Pop M, Salzberg SL. 2009. Ultrafast and memory-efficient alignment of short DNA sequences to the human genome. *Genome Biol* **10**: R25.

Li H, Handsaker B, Wysoker A, Fennell T, Ruan J, Homer N, Marth G, Abecasis G, Durbin R, Genome Project Data Processing S. 2009. The Sequence Alignment/Map format and SAMtools. *Bioinformatics* **25**: 2078-2079.

Love MI, Huber W, Anders S. 2014. Moderated estimation of fold change and dispersion for RNA-seq data with DESeq2. *Genome Biol* **15**: 550.

Robinson JT, Thorvaldsdottir H, Winckler W, Guttman M, Lander ES, Getz G, Mesirov JP. 2011. Integrative genomics viewer. *Nat Biotechnol* **29**: 24-26.

Szklarczyk D, Franceschini A, Wyder S, Forslund K, Heller D, Huerta-Cepas J, Simonovic M, Roth A, Santos A, Tsafou KP et al. 2015. STRING v10: protein-protein interaction networks, integrated over the tree of life. *Nucleic Acids Res* **43**: D447-452.

Thorvaldsdottir H, Robinson JT, Mesirov JP. 2013. Integrative Genomics Viewer (IGV): high-performance genomics data visualization and exploration. *Brief Bioinform* **14**: 178-192.

Trapnell C, Pachter L, Salzberg SL. 2009. TopHat: discovering splice junctions with RNA-Seq. *Bioinformatics* **25**: 1105-1111.

Trapnell C, Williams BA, Pertea G, Mortazavi A, Kwan G, van Baren MJ, Salzberg SL, Wold BJ, Pachter L. 2010. Transcript assembly and quantification by RNA-Seq reveals unannotated transcripts and isoform switching during cell differentiation. *Nat Biotechnol* **28**: 511-515.

Figure S1

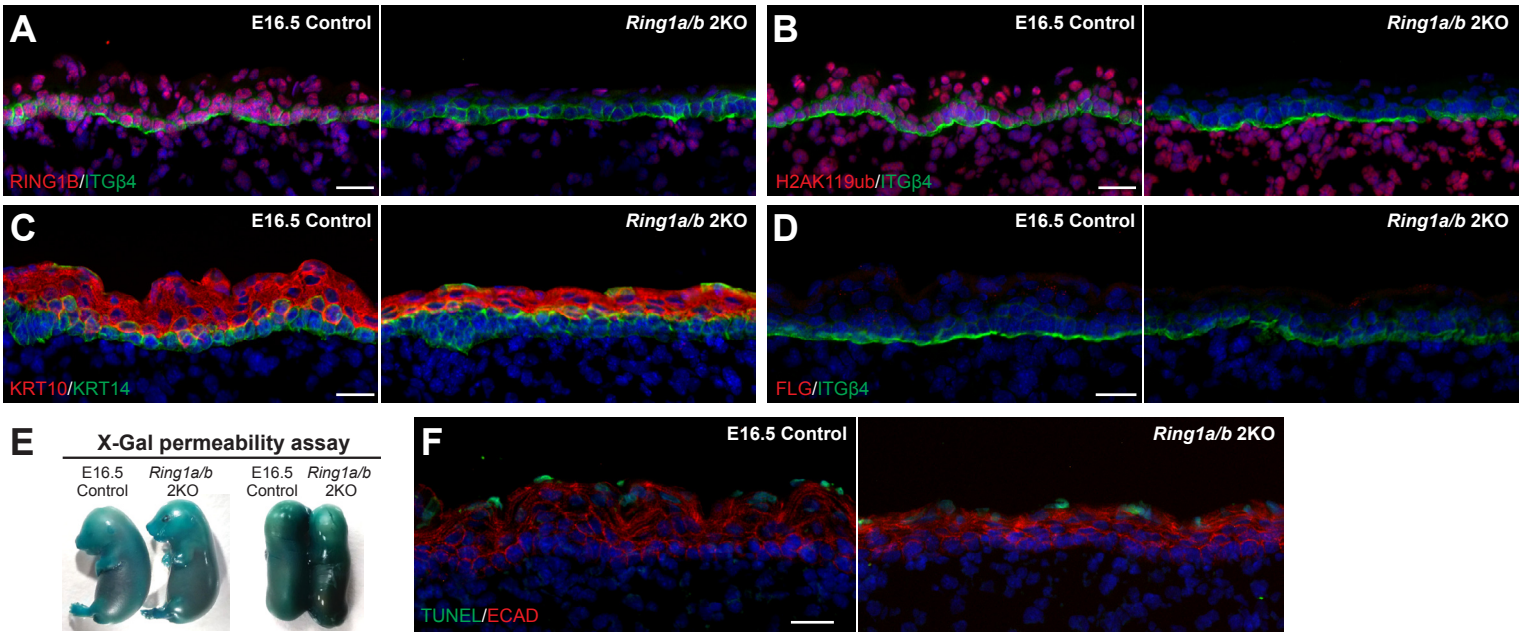

Figure S1. *Ring1a/b* 2KO epidermis displays normal epidermal stratification program. (**A**) Immunofluorescence staining for RING1B (red) confirming loss of RING1B in *Ring1a/b* 2KO skin epithelium at E16.5. Basement membrane is labeled by ITGβ4 (green). Scale, 25μm. (**B**) Immunofluorescence staining for H2AK119ub (red) confirming loss of H2AK119ub in *Ring1a/b* 2KO skin epithelium at E16.5. Basement membrane is labeled by ITGβ4 (green). Scale, 25μm. (**C**) Immunofluorescence staining for the basal layer marker keratin (KRT) 14 (green) and the differentiated suprabasal layers marker KRT10 (red). Scale, 25μm. (**D**) Immunofluorescence staining for the late differentiation marker FLG (red). Basement membrane is labeled by ITGβ4 (green). Scale, 25μm. (**E**) X-gal skin permeability assay in E16.5 *Ring1a/b* 2KO and control mice. (**F**) TUNEL assay (green) for apoptosis in *Ring1a/b* 2KO skin epithelium compared to control. Skin epithelium is labeled by E-cadherin (ECAD), red. Note TUNEL(+) cells in the upper differentiated layers undergoing terminal differentiation and programed cell death. Scale, 25μm.

Figure S1

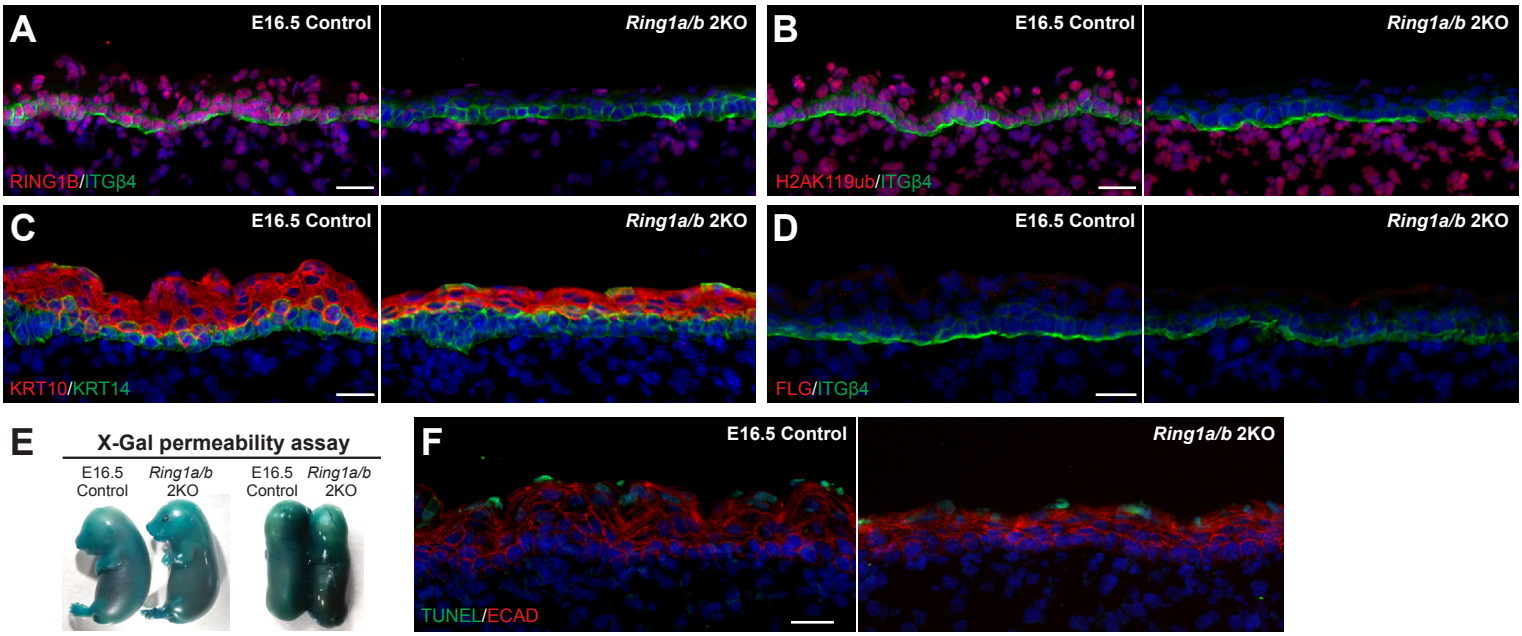

Figure S1. *Ring1a/b* 2KO epidermis displays normal epidermal stratification program. (**A**) Immunofluorescence staining for RING1B (red) confirming loss of RING1B in *Ring1a/b* 2KO skin epithelium at E16.5. Basement membrane is labeled by ITGβ4 (green). Scale, 25μm. (**B**) Immunofluorescence staining for H2AK119ub (red) confirming loss of H2AK119ub in *Ring1a/b* 2KO skin epithelium at E16.5. Basement membrane is labeled by ITGβ4 (green). Scale, 25μm. (**C**) Immunofluorescence staining for the basal layer marker keratin (KRT) 14 (green) and the differentiated suprabasal layers marker KRT10 (red). Scale, 25μm. (**D**) Immunofluorescence staining for the late differentiation marker FLG (red). Basement membrane is labeled by ITGβ4 (green). Scale, 25μm. (**E**) X-gal skin permeability assay in E16.5 *Ring1a/b* 2KO and control mice. (**F**) TUNEL assay (green) for apoptosis in *Ring1a/b* 2KO skin epithelium compared to control. Skin epithelium is labeled by E-cadherin (ECAD), red. Note TUNEL(+) cells in the upper differentiated layers undergoing terminal differentiation and programed cell death. Scale, 25μm.

Figure S2

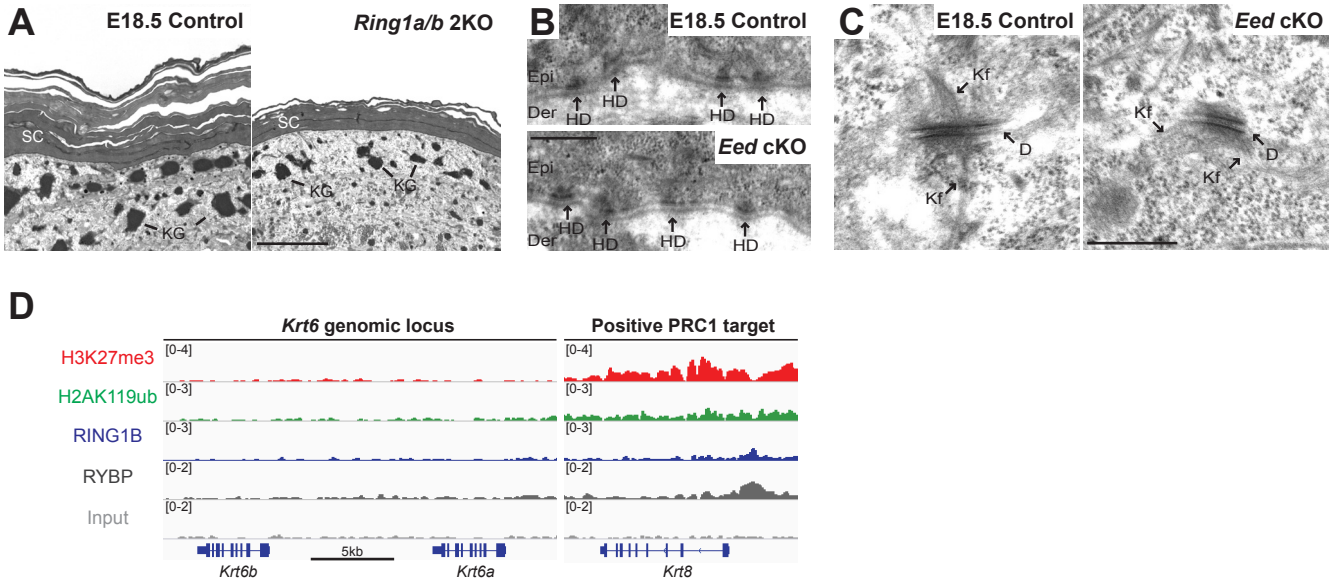

Figure S2. Ultrastructural analysis of *Ring1a/b* 2KO and *Eed* cKO epidermis. (**A**) TEM ultrastructural analysis of differentiated epidermis layers in control and *Ring1a/b* 2KO skins. Note the presence of keratohyalin granules and stratum corneum in *Ring1a/b* 2KO epidermis. Scale, 5µm. (**B-C**) TEM ultrastructural analyses of control and *Eed* cKO skins. (**B**) High magnification of epidermal basement membrane region. Scale, 0.5µm. (**C**) High magnification of cell-cell adhesion region between basal and spinous layers of skin epidermis. Scale, 0.5µm. (**D**) IGV browser views of RING1B, H2AK119ub, H3K27me3, RYBP and input for *Krt6a* and *Krt6b* genes, encoding for KRT6 that is ectopically induced in *Ring1a/b* 2KO compared to control epidermis. *Krt8* gene serves as a positive PRC1 target gene. Der, dermis; SC, stratum corneum; HD, hemi-desmosome; D, desmosome; Kf, keratin intermediate fillaments; KG, keratohyalin granules.

Figure S3

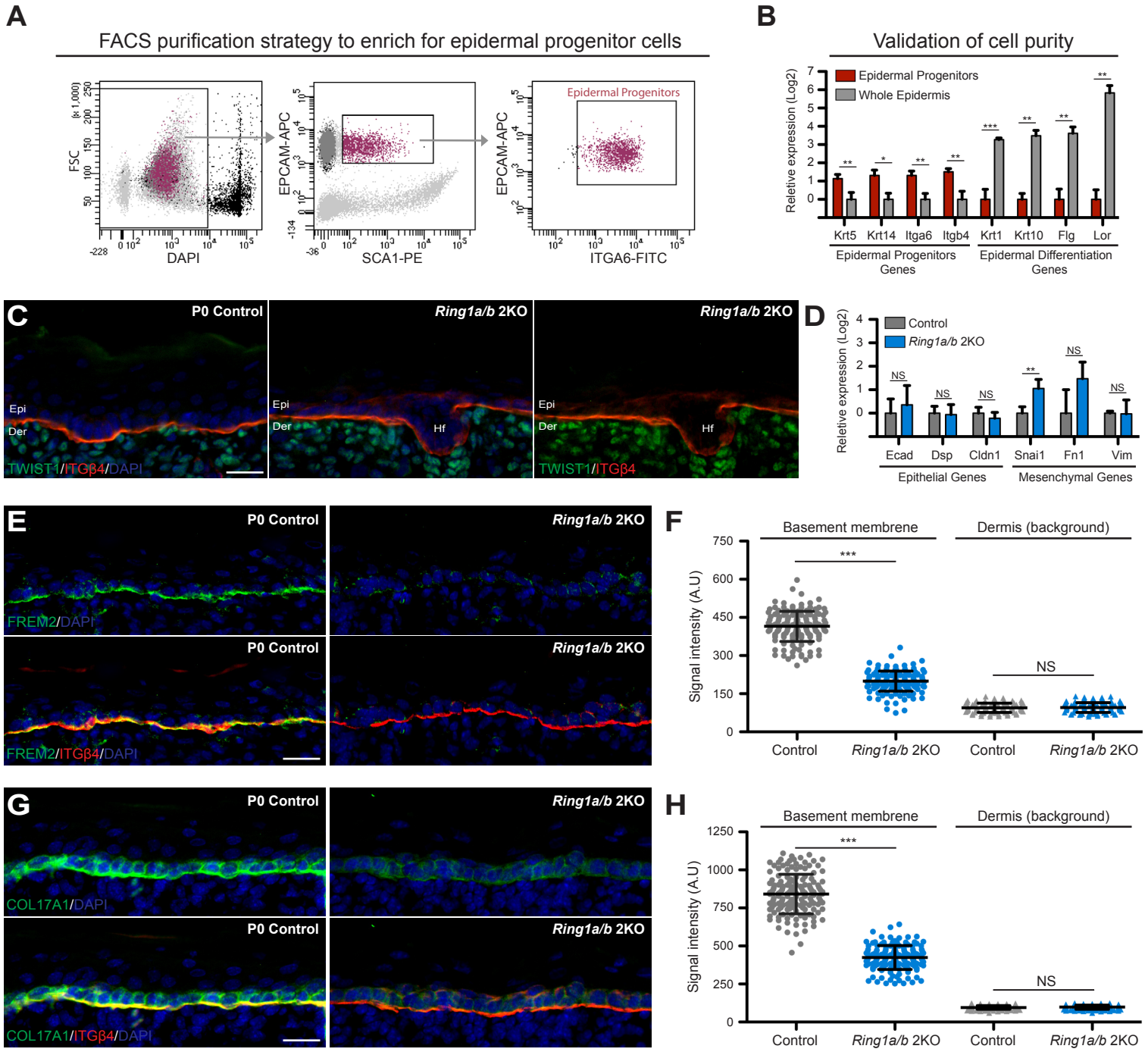

Figure S3. PRC1 preserves transcriptional identity in skin epidermis. (**A**) FACS strategy for purification of basal layer cells enriched for epidermal progenitors from the back skin of P0 mice. Dead cells were excluded by DAPI staining. Then, epidermal cells were selected by SCA1 and EPCAM staining. Basal layer cells enriched for epidermal progenitors were purified as SCA1+ EPCAM+ ITGα6^{hi} (**B**) RT-qPCR analysis validates the FACS sorting strategy and shows enrichment of epidermal progenitors over pre-sorted whole epidermis cells. Note enrichment in the expression of cell-type-specific genes in corresponding populations. Data are mean ±SEM, n=3. *p<0.05, **p<0.01, ***p<0.001 (two-sided t test) (**C**) Immunofluorescence staining for TWIST1 (green). Basement membrane is labeled by ITGβ4 (red). Scale, 25μm. (**D**) RT-qPCR analysis for epithelial and mesenchymal genes in *Ring1a/b* 2KO vs. control epidermal cells. Data are mean ±SD, n=3. **p<0.01; NS, not significant (two-sided t test). (**E**) Immunofluorescence staining for FREM2 (green). Basement membrane is labeled by ITGβ4 (red). Scale, 25μm. (**F**) Quantification of FREM2 staining intensity. Background staining intensity was measured in dermal regions within the same image. Intensity is shown as arbitrary units (A.U). Data are scatter dot plots with mean ±SD. Number of animals for each condition, N=3. ***p<0.01; NS, not significant (Mann-Whitney test). (**G**) Immunofluorescence staining for COL17A1 (green). Basement membrane is labeled by ITGβ4 (red). Scale, 25μm. (**H**) Quantification of COL17A1 staining intensity. Background staining intensity was measured in dermal regions within the same image. Intensity is shown as arbitrary units (A.U). Data are scatter dot plots with mean ±SD. Number of animals for each condition, N=3. ***p<0.01; NS, not significant (Mann-Whitney test).

Figure S4

A

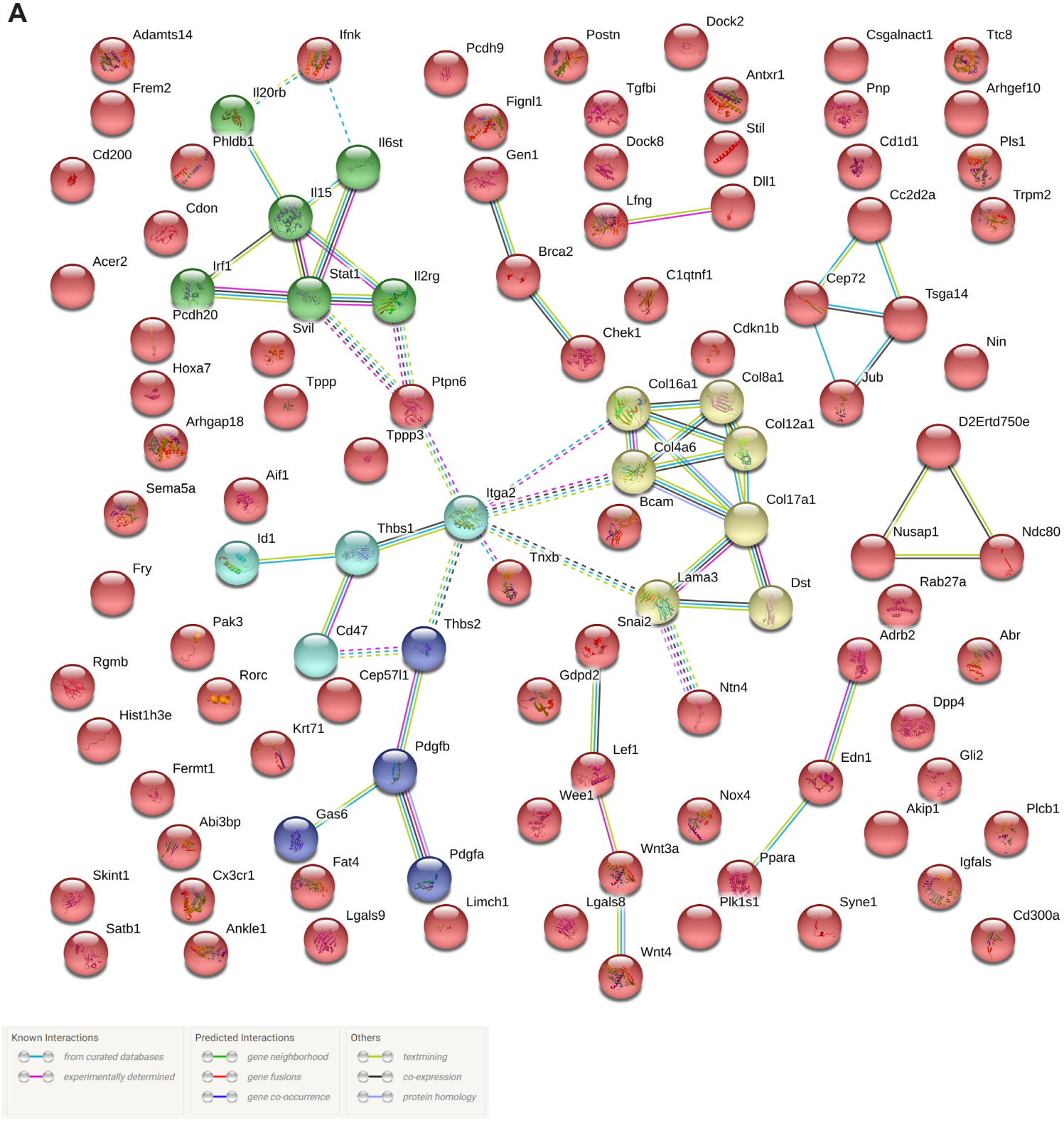

Figure S4. STRING protein-protein interaction analysis. (**A**) STRING protein-protein connectivity network of *Ring1a/b* 2KO downregulated genes related to cell adhesion and cytoskeleton organization. Confidence interaction score threshold was set at 0.7 (high confidence), using k-means clustering method with 5 clusters. Network contains 55 edges (vs. 10 expected edges); Average local clustering coefficient: 0.257; PPI enrichment p-value < 10^{-16}.

Figure S5

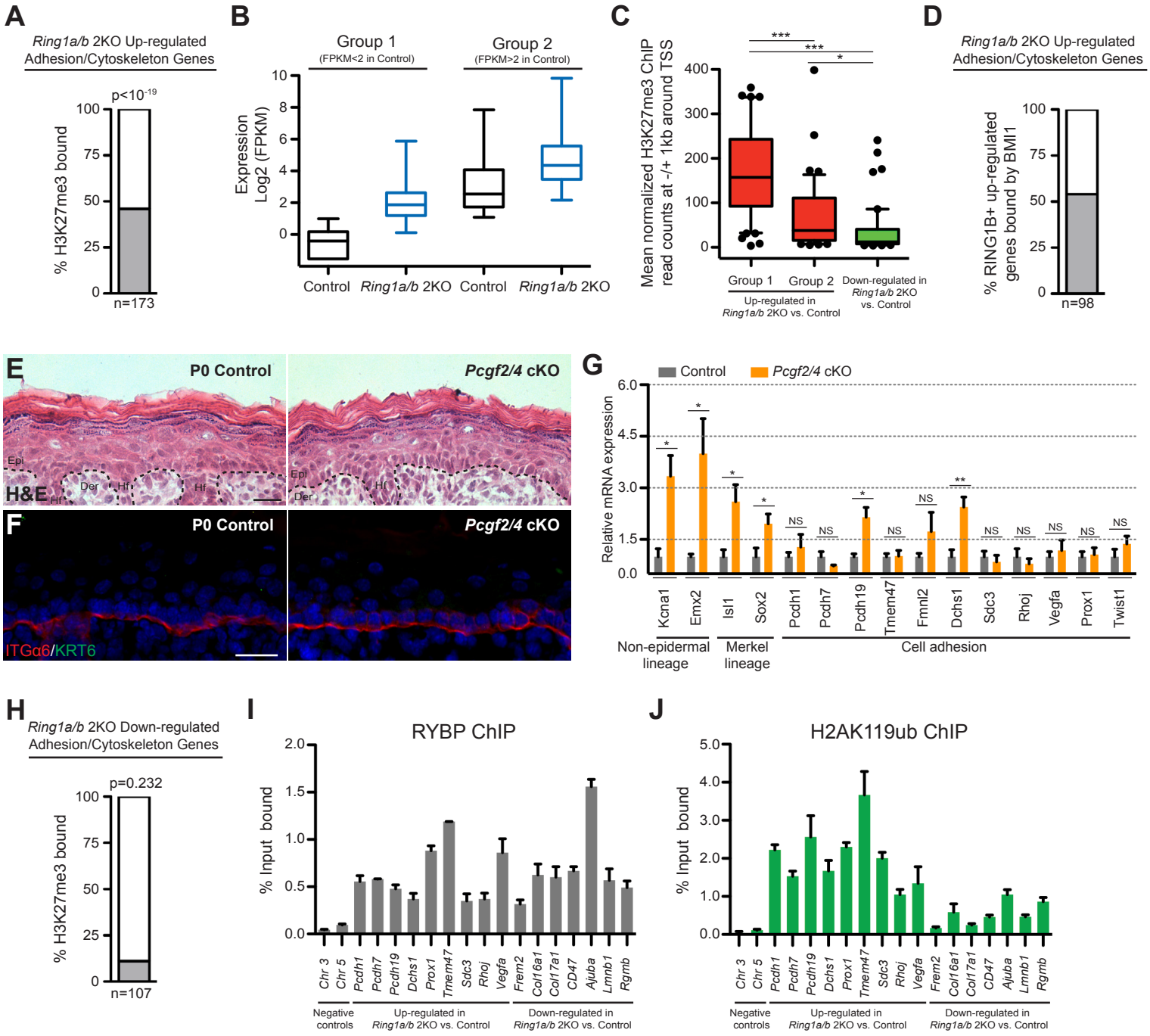

Figure S5. PRC1 regulates cell adhesion and cytoskeleton organization genes (**A**) Percentage of *Ring1a/b* 2KO up-regulated genes related to cell adhesion and cytoskeleton organization, with H3K27me3 ChIP-seq peaks (**B**) Box plots show the mean expression of up-regulated genes related to adhesion and cytoskeleton that are bound by RING1B, in control (black) and *Ring1a/b* 2KO (blue) epidermis. Group 1 genes defined as mean expression of FPKM<2. Group 2 genes defined as mean expression of FPKM≥2. Box and whisker boxplots are minimum to maximum: midline, median; box limits, 25th percentile (lower quartile) and 75th percentile (upper quartile); upper whisker, 75th-100th percentile; lower whisker, 0-25th percentile. (**C**) Boxplots show H3K27me3 ChIP-seq read counts in control epidermis at ±1kb around TSS, for indicated groups of genes. Box and whisker boxplots are 10th-90th percentile: midline, median; box limits, 25th percentile (lower quartile) and 75th percentile (upper quartile); upper whisker, 75th-90th percentile; lower whisker, 10-25th percentile. Data outside boxplot limits are presented as outliers. (**D**) Proportion of BMI1-bound genes among RING1B(+) up-regulated genes related to cell adhesion and cytoskeletal organization. (**E**) H&E analysis of *Pcgf2/4* cKO mice compared to control skins. Scale, 25μm. (**F**) Immunofluorescence staining for KRT6 (green). Basement membrane is labeled by ITGα6 (red). Scale, 25μm. (**G**) RT-qPCR analysis *Pcgf2/4* cKO compared to control epidermal cells. Data are mean ±SEM, n=3. *p<0.05; **p<0.01; ***p<0.001; NS, not significant (two-sided t test). (**H**) Percentage of *Ring1a/b* 2KO down-regulated genes related to cell adhesion and cytoskeleton organization, with H3K27me3 ChIP-seq peaks (**I-J**) ChIP-qPCR showing the binding of RYBP (**I**) and H2AK119ub (**J**) in control epidermis. Data are mean ±SEM, n=2.

Figure S6

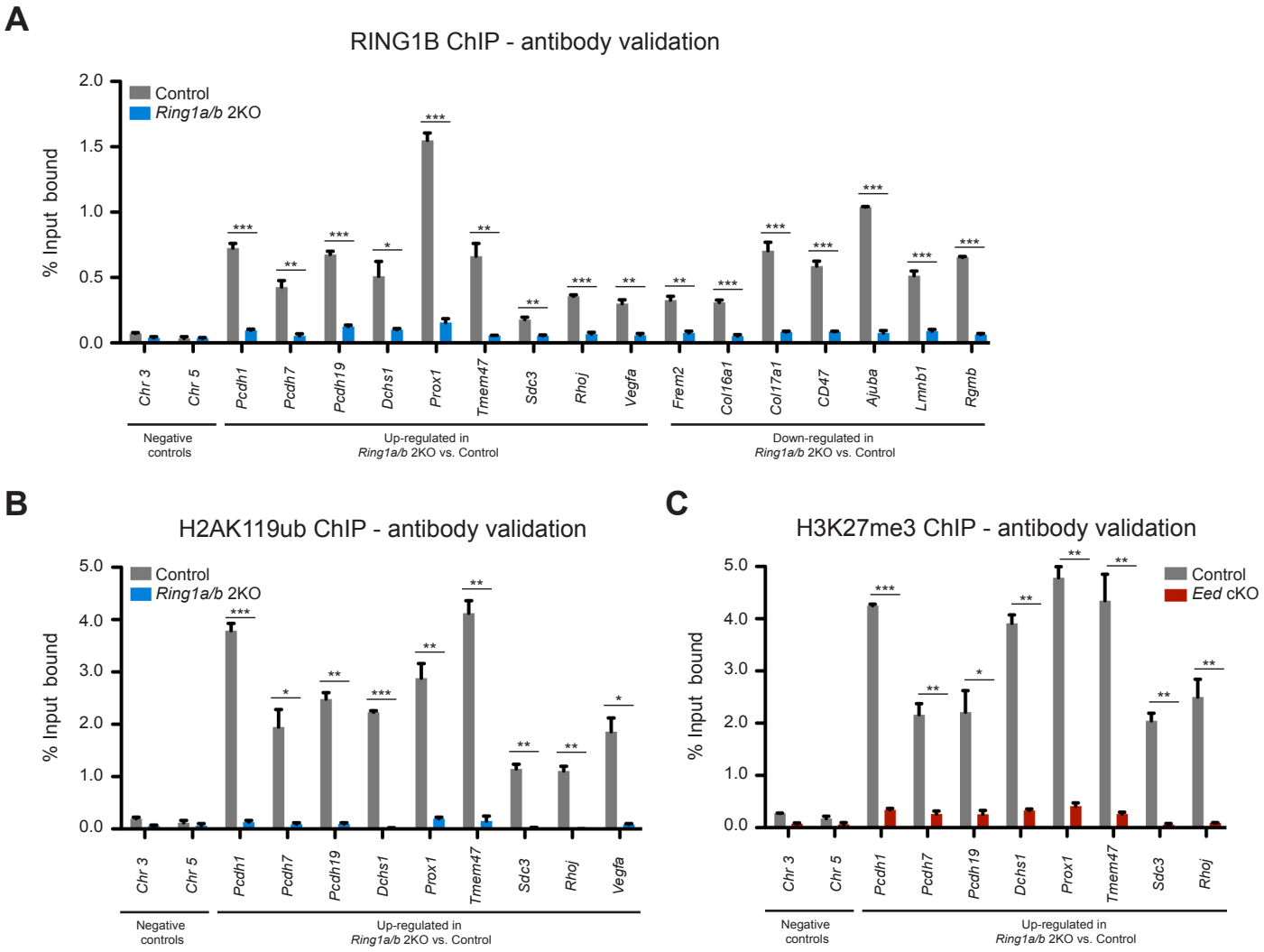

Figure S6. Validation of chromatin immunoprecipitation (ChIP) antibodies. (**A**) ChIP-qPCR showing the binding of RING1B in *Ring1a/b* 2KO and control epidermis. Data are mean ±SEM, n=3. *p<0.05; **p<0.01; ***p<0.001 (two-sided t test). (**B**) ChIP-qPCR showing the binding of H2AK119ub in *Ring1a/b* 2KO and control epidermis. Data are mean ±SEM, n=2. *p<0.05; **p<0.01; ***p<0.001 (two-sided t test). (**C**) ChIP-qPCR showing the binding of H3K27me3 in *Eed* cKO and control epidermis. Data are mean ±SEM, n=2. *p<0.05; **p<0.01; ***p<0.001 (two-sided t test).